Chapter 2

Analysis of metabolites in the terpenoid pathway of *Catharanthus roseus* cell suspensions

Mohd Zuwairi Saiman[1,2], Natali Rianika Mustafa[1,3], Barbora Pomahačová[3], Marianne Verberne[1], Robert Verpoorte[1], Young Hae Choi[1], Anna Elisabeth Schulte[1,3]

[1]Natural Products Laboratory, Institute of Biology, Leiden University, 2300 RA Leiden, The Netherlands

[2]Institute of Biological Sciences, Faculty of Science, University of Malaya, 50603 Kuala Lumpur, Malaysia

[3]ExPlant Technologies B.V., Galileiweg 8 2333 BD Leiden, The Netherlands

Published in Plant Cell Tiss Organ Cult (2014) 117: 225–239

Abstract

In *Catharanthus roseus* cell cultures, the monoterpenoid pathway has been shown to be a limiting factor in terpenoid indole alkaloid (TIA) production. This could be due to competition at the level of isopentenyl diphosphate::dimethylallyl diphosphate (C5) which leads to the biosynthesis of different terpenoid groups. For future engineering of the terpenoid pathway, chemical characterization of *C. roseus* cell cultures is a necessity. Therefore, in this study nine *C. roseus* cell suspension lines were characterized by analyzing the levels of the major terpenoids derived from different biosynthetic pathways which may compete for the same precursors; TIA (monoterpenoid, C10), carotenoids (tetraterpenoid, C40), and sterols (triterpenoid, C30). Among the cell lines, CRPP (S) was the most promising TIA-producing cell line which provided more TIA (24 µmol/g DW) than carotenoids (15 µmol/g DW) and sterols (2 µmol/g DW). However, when considering the distribution of the isopentenyl-precursor (C5), the carotenoids which assemble from 8 x C5 represent twofold more C5-units (122 µmol/g DW) than the TIA in this cell line. In the CRPP (G), A12A2 (G), and A12A2 (S) cell lines, the C5 distribution was predominant towards carotenoid biosynthesis as well, resulting in a relatively high accumulation of carotenoids. The geranylgeranyl diphosphate (C20) pathway towards carotenoid production is therefore considered competitive towards TIA biosynthesis. For channeling more precursors to the TIA, the branch point for C10 and C20 seems an interesting target for metabolic engineering. Using principal component analysis of the chromatographic data, we characterized the cell lines chemically based on their metabolite levels. The information on the metabolic composition of *C. roseus* cell cultures is useful for developing strategies to engineer the metabolic pathways and for selection of cell lines for future studies.

Introduction

Catharanthus roseus (Apocynaceae) produces more than 130 terpenoid indole alkaloids (TIA), including the antihypertensive monomeric alkaloids ajmalicine and serpentine, as well as some bisindole alkaloids, such as the anticancer agents vinblastine and vincristine (van der Heijden et al. 2004). Terpenoid indole alkaloids in *C. roseus* are biosynthesized from the central intermediate strictosidine, a product of condensation between the aldehyde function of the iridoid secologanin and the amino group of the indole tryptamine. Tryptamine derives from the shikimate pathway, whereas the iridoid moiety originates from 10-hydroxygeraniol (also known as 8-hydroxygeraniol) after hydroxylation of geraniol produced from geranyl diphosphate (GPP; C10) (El-Sayed and Verpoorte 2007;

Salim and De Luca 2013; **Fig. 1**). Geranyl diphosphate is synthesized from isopentenyl diphosphate (IPP) and its isomer dimethylallyl diphosphate (DMAPP), which is subject to further condensation, thus generating farnesyl diphosphate (FPP; C15), and geranylgeranyl diphosphate (GGPP; C20). Farnesyl diphosphate leads to the formation of triterpenoids (sterols; C30) and sesquiterpenoids (C15), while GGPP leads to the production of diterpenoids (C20) and tetraterpenoids (carotenoids; C40) (Rohmer 1999; **Fig. 1**).

The two terpenoid building blocks, IPP and DMAPP can be produced via two distinct metabolic routes, i.e. the mevalonate (MVA) pathway in cytosol and the 2-*C*-methyl-D-erythritol 4-phosphate (MEP) pathway in plastids (Rohmer 1999). In plants, both MVA and MEP pathways coexist, while active in different subcellular compartments, each leading to a distinct set of terpenoid derivatives (**Fig. 1**). However, there is evidence of cross-talk between the IPP::DMAPP pools even though the MVA and MEP pathways are present in different cellular compartments in plant cells (Rohmer 1999; Hemmerlin et al. 2003; Schuhr et al. 2003; Laule et al. 2003). In addition, the MVA pathway has a regulatory effect on the MEP pathway by the activation of some of MEP pathway genes (Courdavault et al. 2005).

The generation of IPP::DMAPP and GPP and its distribution into different biosynthetic routes is of specific interest as they are precursors of the monoterpenoid geraniol, from which secologanin and the pharmaceutically important TIA are derived in *C. roseus*. The production levels of the bisindole alkaloids in *C. roseus* are low, which limits availability, resulting in high market prices (van der Heijden et al. 2004; Zhou et al. 2009). Plant cell cultures have been used as a potential continuous and reliable source of the bioactive metabolites (Moreno et al. 1995; van der Heijden et al. 2004; Pietrosiuk et al. 2007; Pati et al. 2010). Despite efforts to optimize growing and production conditions, large-scale cultivation of *C. roseus* cells for commercial production of TIA has not yet been obtained (Moreno et al. 1995; van der Heijden et al. 2004; Zhao and Verpoorte 2007).

Engineering of metabolic pathways has a great potential to enhance the metabolic fluxes into the TIA pathway, thus increasing feasibility for commercial production of TIA by plant cell and tissue cultures (Verpoorte et al. 2002; Zhao and Verpoorte 2007; Zhou et al. 2009; O'Connor 2012; Glenn et al. 2013). Based on feeding studies in *C. roseus* cell cultures, the terpenoid pathway has been shown to be a limiting factor in TIA production (Moreno et al. 1993; Whitmer et al. 2002; van der Heijden et al. 2004; Zhao and Verpoorte 2007). This could be due to a lack of precursors/intermediates, associated with low gene expression or enzyme activity in the MEP pathway, and/or it might be due to competition at the level of IPP::DMAPP and GPP with conversion steps favoring either geraniol and derived

monoterpenoids, versus GGPP and derived carotenoids and/or FPP and derived sterols. Chemical characterization of *C. roseus* cell cultures will provide important information on their metabolic composition and a better understanding of the possible changes induced during the experiments, both of which are prerequisite to engineer the metabolic pathway.

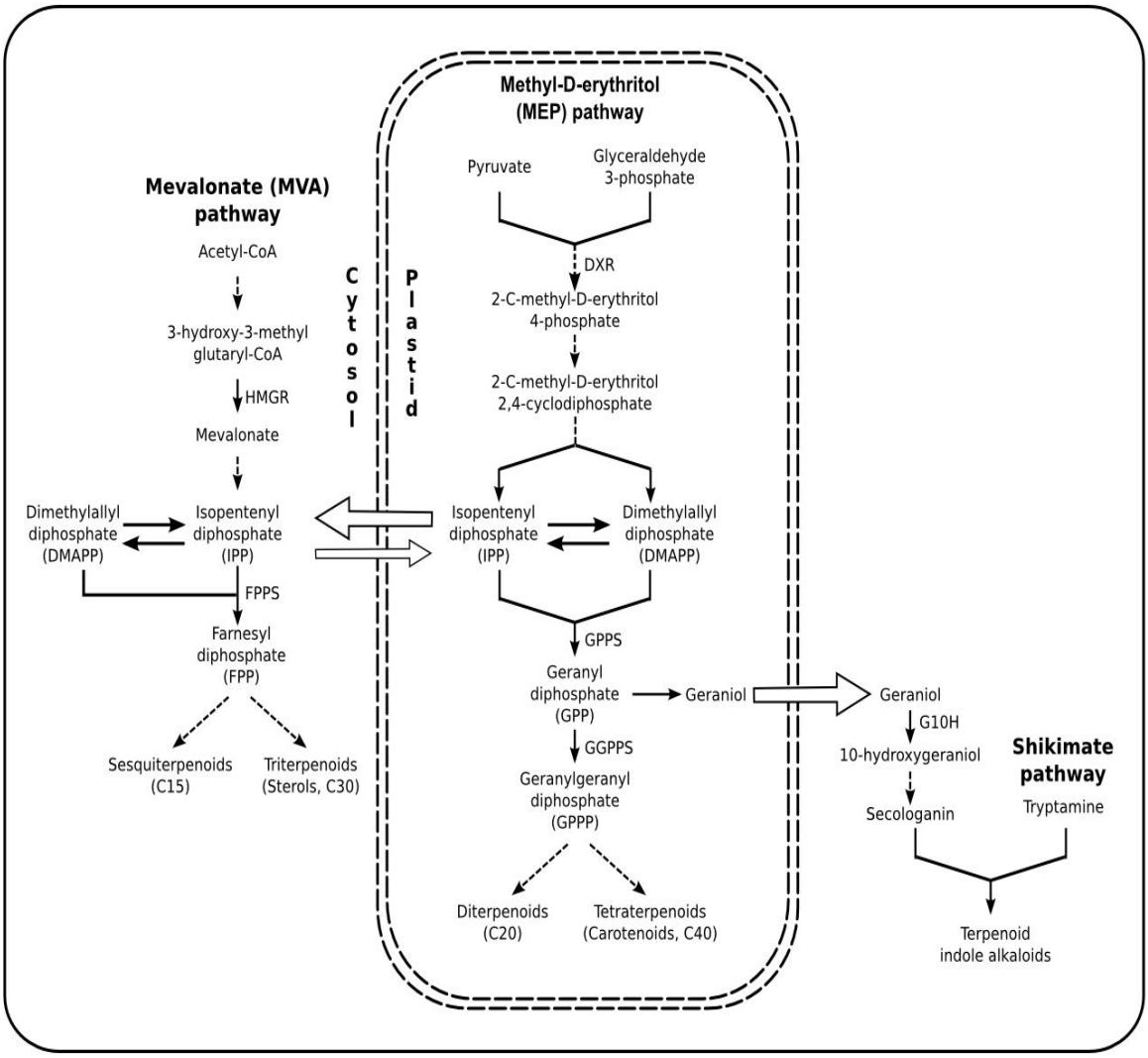

Fig. 1 The terpenoid biosynthetic pathway localized in cytosol and plastid generate different groups of terpenoid (adapted from Laule et. al 2003). Arrows with dashed lines indicate several biosynthetic steps. DXR: 1-deoxy-D-xylulose-5-phosphate reducto isomerase, FPPS: farnesyl diphosphate synthase, G10H: geraniol 10-hydroxylase (G8O: geraniol 8-oxidase), GPPS: geranyl diphosphate synthase, GGPPS: geranylgeranyl diphosphate synthase, HMGR: 3-hydroxy-3-methylglutaryl-CoA reductase.

Most characterization studies of *C. roseus* cell cultures have been focused on TIA production with little attention given to other metabolite groups in associated biosynthetic pathways that might compete for the same precursors. In this study, nine *C. roseus* cell suspension lines were analyzed for their production levels of TIA, iridoid and indole

precursors, as well as the sterols and carotenoids as the major representatives of triterpenoid and tetraterpenoid groups, respectively. Furthermore, the total accumulation of TIA, carotenoids, and sterols and the distribution of five-carbon (C5) precursors among the different terpenoid groups were evaluated. The metabolite data were also analyzed using principal component analysis (PCA) to determine which metabolites are responsible in discriminating the cell lines. In addition, the mRNA transcription levels of some representative genes of the associated terpenoid pathways were profiled.

The objective of the present study was to characterize several *C. roseus* cell lines for accumulation of major chemical groups derived from the different terpenoid biosynthetic pathways and to identify candidate lines with a high TIA-producing capacity for further in depth studies to enhance channeling of the C5 precursors towards the TIA.

Materials and methods

Plant cell cultures

The cell lines of *C. roseus* suspension cultures were developed in the past 20 years and maintained in the Natural Products Laboratory, Institute of Biology, Leiden University, The Netherlands. Nine cell lines used for this study were labeled as A12A2 (G), A12A2 (S), CRPP (G), CRPP (S), A11 (G), A11 (S), CRPM (G), CRPM (S), and CATL (S) (Mustafa et al. 2011). Some of them have been employed in the studies of terpenoid indole alkaloid, phenylpropanoid and salicylic acid pathways. The cell lines were grown in MS (Murashige and Skoog 1962) or B5 (Gamborg et al. 1968) medium supplemented with either 20 g/l glucose (G) or 30 g/l sucrose (S) in 250 ml Erlenmeyer flasks with 100 or 70 ml culture volume per flask. The cell cultures were maintained for more than ten years as batch suspension cultures subcultured every 7 – 21 days by taking various ratios of cells to fresh medium, depending on the line. Vitamin and growth regulator requirements varied with the lines (see **Table 1** for the cell line characteristics). Flasks were closed with T-32 silicon foam stoppers (Shin Etsu, Tokyo, Japan) and placed on a gyratory shaker (110 rpm) at 25 ± 1 ^{o}C under continuous light (10.8 – 27 µE/m^2/sec).

Table 1 Characteristics of *Catharanthus roseus* cell suspension lines employed in the study (Natural Products Laboratory, Institute of Biology,Leiden University, The Netherlands)

Cell Lines[a]	Medium[b]	Growth cycle (days)	Method Subculture	Phenotype	Description
A12A2 (G)	MS; with thiamine (1 mg/l), glucose (20 g/l), pH 5.8	7	1:1 dilution of 100 ml culture into 100 ml medium and divided to two flasks	Green cells, micro aggregates	• The A12A2 cell line derived from 9CR58 cell line, which was the habituated version of the original cell line 58CR. The parent culture was initiated from seeds in 1983. Then, the A12A2 cells have been maintained in Murashige and Skoog (MS) medium deprived from growth hormones and supplemented with 30 g/l sucrose (Moreno et al. 1993) or 20 g/l glucose. • The A12A2 cell line was used in several experiments and reported to accumulate tryptamine, strictosidine, ajmalicine (Moreno et al. 1993; El-Sayed and Verpoorte, 2002). • It is a high salicylic acid production cell line, which accumulate 2,3-dihydroxybenzoic acid after a fungal elicitation (Mustafa and Verpoorte 2007) and 2,5-dihydroxybenzoic acid glucoside after salicylic acid elicitation (Mustafa et al. 2009). • Collu et al. (2002) used A12A2 cell line to study the relationship between G10H (G8O) and alkaloid accumulation.
A12A2 (S)	MS; with thiamine (1 mg/l), sucrose (30 g/l), pH 5.8	14	Transfer 20 ml culture into 50 ml medium	Green cells, micro aggregates	
CRPP (G)	B5; with NAA (1.86 mg/l), glucose (20 g/l), pH 5.8	21	1:1 dilution of 100 ml culture into 100 ml medium and divided to two flasks	Dark green cells, micro aggregates	• The CRPP cell line was initiated in 1993 from *C. roseus* cv. Pacifica Punch. • It produced lower level of salicylic acid than the A12A2 cell line upon fungal elicitation.
CRPP (S)	B5; with NAA (1.86 mg/l), sucrose (30 g/l), pH 5.8	21	Transfer 20 ml culture into 50 ml medium	Dark green cells, micro aggregates	
A11 (G)	B5; with NAA (1.86 mg/l), glucose (20 g/l), pH 5.8	14	1:1 dilution of 100 ml culture into 100 ml medium and divided to two flasks	Green aggregates	• The A11 cell line derived from 9CR58 cell line, which was originated from 58CR cell line by changing to B5 medium supplemented with 1.86 mg/l NAA and 20 g/l sucrose. • A11 cell line had been used for studying the iridoid biosynthesis and reported to

A11 (S)	B5; with NAA (1.86 mg/l), sucrose (30 g/l), pH 5.8	14	Transfer 20 ml culture into 50 ml medium	Green-yellowish cells, micro aggregates	accumulate secologanin rather than tryptamine (Contin et al. 1999). • A11 cells produced G10H (G8O), strictosidine, and ajmalicine (5-, 10- and 2.5-fold, respectively) higher than the A12A2 cells (Contin et al. 1999).
CRPM (G)	MS; with thiamine (0.4 mg/l), no pyridoxine, no nicotinic acid, no glycine, NAA (2 mg/l), kinetin (0.2 mg/l), glucose (20 g/l), pH 5.8	7	1:1 dilution of 100 ml culture into 100 ml medium and divided to two flasks	Creamy fine cells	• The CRPM cell line derived from 58CR cell line. • It was used to study the G10H (G8O) activity (Collu et al. 2002) • It was a successful model for transformation of isochorismate synthase gene (Mustafa and Verpoorte 2007). • It produced a high number of vacuoles and was used as a model for studying vacuolar transportation. It is also a suitable cell line for protoplast isolation.
CRPM (S)	MS; with thiamine (0.4 mg/l), no pyridoxine, no nicotinic acid, no glycine, NAA (2 mg/l), kinetin (0.2 mg/l), sucrose (30 g/l), pH 5.8	7	Transfer 20 ml culture into 50 ml medium	Creamy fine cells	
CATL (S)	MS; with NAA (2 mg/l), kinetin (0.2 mg/l, sucrose (30 g/l), pH 5.8	7	Transfer 20 ml culture into 50 ml medium	Yellowish fine cells	• The CATL cell line derived from MP183L cell line, which was originated from A12A2 cell line. • Its parent cell line MP183L was used for protoplast isolation and transformation.

NAA: 1-naphthaleneacetic acid
G10H (G8O): geraniol 10-hydroxylase (also known as geraniol 8-oxidase)
[a]G or S in brackets indicates that the cell lines were grown with glucose or sucrose at 20 or 30 g/l, respectively in the medium.
[b]Except when mentioned otherwise, the medium composition (macro- and micro-nutrients, iron, and vitamins) is according to the MS: Murashige and Skoog (1962); or B5: Gamborg et al. (1968).

Harvesting

Three replicate flasks of each cell line were harvested at the end of their growth cycle (see **Table 1** for growth cycle length), at which the cells were in the stationary phase. The cells were filtered under reduced pressure using a Bűchner funnel. Subsequently, the cells were washed with deionized water, frozen in liquid nitrogen, and lyophilized for 72 hours. The dried cells were kept at room temperature in the dark until further analysis.

Analysis of terpenoid indole alkaloids and precursors

The extraction was adapted from Moreno et al. (1993). Freeze-dried cells (100 mg) from triplicate flasks of each cell lines were extracted two times with 5 ml methanol, vortexed for 10 sec, ultrasonicated for 20 min, and centrifuged at 3,500 rpm for 30 min. The

supernatant was pooled and concentrated to dryness under reduced pressure. The residue was resuspended in 1 ml of 1 M phosphoric acid (H_3PO_4), vortexed for 10 sec, and centrifuged at 13,000 rpm for 10 min. The supernatant was filtered through miracloth before analysis.

Two separate methods for analysis of TIA and TIA precursors were adapted from Tikhomiroff and Jolicoeur (2002). Method **1** was applied for the analysis of TIA (strictosidine, ajmalicine, serpentine, catharanthine, tabersonine, vindoline, vinblastine, and vincristine) using high-performance liquid chromatography (HPLC) on an Agilent Technologies 1200 series chromatograph (Agilent Technologies Inc., Santa Clara, CA, USA). The mobile phase of method **1** consisted of 5 mM Na_2HPO_4 (pH adjusted to 6 with H_3PO_4) (solvent A) and acetonitrile (solvent B). The eluent profile (volume of solvent A/volume of solvent B) was: 0 – 20 min, linear gradient from 80:20 to 20:80; 20 – 25 min, isocratic elution with 20:80 (v/v); 25 – 30 min, linear gradient from 20:80 to 80:20; 30 – 31 min, isocratic elution with 80:20 (v/v). Method **2** was applied for the analysis of TIA precursors (tryptophan, tryptamine, loganic acid, loganin, and secologanin) using a Waters HPLC system (Waters, Milford, MA, USA). The mobile phase of method **2** was 0.01 M H_3PO_4–acetonitrile (85:15, v/v) (isocratic elution). Both methods **1** and **2** were carried out using a Zorbax Eclipse XDB-C18 column (250 mm x 4.6 mm, particle size 5µ) (Agilent Technologies Inc.). The flow rate was 1.5 ml/min and the injection volume was 50 µl for both chromatographic methods. Peak identification was based on a comparison of the retention time and the UV spectrum of the target peaks with those of the standard compounds. Calibration curves of the standard compounds were made for quantitative analysis.

Analysis of carotenoids

Samples were extracted as described by Bino et al. (2005) with some modifications: 70 – 100 mg freeze-dried cells from triplicate flasks of each cell line were extracted with 6 ml of a mixture of methanol, chloroform containing 0.1% butylated hydroxytoluene (BHT) (w/v), and water, in a ratio of 6:5:1 (v/v). The mixture was vortexed for 1 min and left on ice in the dark for 10 min. Subsequently, 3 ml of 50 mM Tris buffer (pH 7.5) containing 1 M sodium chloride and 0.1% BHT (w/v) was added, vortexed for 1 min, and left on ice in the dark for 10 min. Then the mixture was centrifuged (2,500 rpm, 4 ºC, 10 min) and the chloroform phase transferred into a clean, dark vial. The residue was extracted two times with 1.5 ml chloroform (containing 0.1% BHT, w/v) and the chloroform phases were pooled. The extraction was concentrated to dryness under nitrogen gas flow and the residue subsequently redissolved in 1 ml methanol, transferred into an Eppendorf tube, and centrifuged at 13,000

rpm for 5 min. The clear supernatant was collected and analyzed by HPLC adapted from Ben-Amotz et al. (1988).

The chromatography system was carried out using a Vydac 201TP54 C18 column (250 mm x 4.6 mm, particle size 5µ) (Grace, Deerfield, IL, USA) and a Waters HPLC system (Waters). The mobile phase was isocratic elution of 100% methanol (HPLC grade) with a flow-rate of 1 ml/min. The injection volume was 40 µl. Peak identification was performed by comparing the retention time and the UV spectra of reference compounds according to Ben-Amotz et al. (1988) and Taylor et al. (1990). Quantitative analysis was based on the calibration curve of lutein or *β*-carotene.

Analysis of phytosterols

Freeze-dried cells (100 mg) from three replicate flasks of each cell line were weighed, except for the CRPM cell lines (50 mg). One ml of 5*α*-cholestan-3*β*-ol (0.25 mg/ml) was added as an internal standard before saponification of the samples with 5 ml of 1 M potassium hydroxide in ethanol–water (95:5, v/v). Subsequently, the samples were vortexed for 10 sec, ultrasonicated for 5 min, and heated at 80 ^{o}C for 30 min. The samples were cooled to room temperature before centrifuging at 3,500 rpm for 5 min. The solvent was transferred into a clean glass tube with addition of 5 ml water, and extracted two times with 5 ml of diethylether–*n*-hexane (1:1, v/v). The upper layers were pooled, evaporated to dryness, and dissolved in 200 µl *n*-hexane. Subsequently, the solution was cleaned with 10 ml of *n*-hexane followed by 5 ml of *n*-hexane–ethylacetate (95:5, v/v) using a BondElut Silica SPE cartridge (Varian Inc., Lake Forest, CA, USA). The latter fraction was collected and evaporated to dryness. The residue was dissolved in 50 µl *n*-hexane, 200 µl pyridine, and 100 µl *N*,*O*-bis(trimethylsilyl)trifluoroacetamide containing 1% trimethylchlorosilane. Subsequently, the mixture was vortexed for 10 sec and heated at 80 ^{o}C for 30 min. The sample was cooled prior to analysis with gas chromatography.

Gas chromatography (GC) equipped with a flame ionization detector (FID) was carried out on an Agilent GC 6890 series (Agilent Technologies Inc.). The column used was a DB-5 (5%-phenyl-methylpolysiloxane) capillary column (30 m length, 0.25 mm internal diameter, film thickness of 0.25 µm) (J&W Scientific Inc., Folsom, CA, USA). The injector temperature was set to 280 ^{o}C, a split ratio of 1:10 and a carrier gas (N_2) flow rate of 1 ml/min. The oven temperature was programmed starting at 200 ^{o}C. The initial temperature began at 200 ^{o}C for 1 min, increased from 200 ^{o}C to 290 ^{o}C at 10 ^{o}C/min and held at 290 ^{o}C for 15 min, providing a total run time of 25 min per sample. The FID detector temperature

was set to 300 ^{o}C. The sample injection volume was 5 µl. Compounds were identified by the retention time compared with those of authentic references. Calibration curves of the standard references were made for quantitative analysis.

Quantitative RT-PCR

Total RNA was isolated from 20 mg of cells and stored at -20^{o}C. DNA contamination was removed using TURBO DNA-free^{TM} kit (Ambion, Carlsbad, CA, USA) according to the manufacturer's instructions. The cDNAs were synthesized from the RNA samples using RevertAid^{TM} (Fisher Scientific, Pittsburgh, PA, USA) oligo (dT) as the primer following the protocol provided by the manufacturer. The cDNAs were used as a template with primers of the specific genes (*HMGR, FPPS, SQS, PDS, DXR, GGPPS, GPS, G10H* or *G8O, TDC, STR, SGD*) listed in **Supplement 1**. The qRT-PCR analysis was performed using a Chromo 4 PTC200 Thermal Cycler (Bio-Rad, Herculas, CA, USA). Ribosomal protein subunit 9 (Rsp9) was used as an internal control and SYBR Green was used in the PCR reactions to quantify the amount of dsDNA. The relative CT (threshold cycle value) method was used to quantify gene expression using MJ Opticon Monitor analysis software version 3.1 (Bio-Rad).

Statistical analysis

Analysis of variance (ANOVA) or *t*-test was performed on SPSS Statistics 17 (SPSS Inc., Chicago, IL, USA) to determine statistical differences ($P < 0.05$). Principal component analysis (PCA) and hierarchical cluster analysis (HCA) were performed on SIMCA-P+ version 12 software (Umetrics, Umeå, Sweden).

Results and Discussion

Analysis of terpenoid indole alkaloids and precursors

The concentrations of terpenoid indole alkaloids (TIA), iridoid and indole precursors in the *C. roseus* cell lines are shown in **Fig. 2**. The indole precursors tryptophan and tryptamine derived from the shikimate pathway were not detected in CRPP (G), CRPP (S) and A11 (S) cell lines, whereas they are found in the other cell lines employed in this study, ranging from 0.14 – 2.97 µmol/g dry weight (DW). Tryptophan (2.97 µmol/g DW) and tryptamine (1.64 µmol/g DW) levels were greater in the CATL (S) compared to the other cell lines ($P < 0.05$). The iridoid precursors, loganin and secologanin were not detected in our cell lines, although the A11 line was previously reported to accumulate secologanin (Contin et al. 1999). However, the precursor of those iridoids, loganic acid was detected in the CRPP

(G) and CRPP (S) cell lines (2.60 – 3.28 µmol/g DW). In addition, both CRPP cell lines accumulated high levels of the alkaloid strictosidine (14.30 – 20.87 µmol/g DW) and serpentine (1.77 – 2.37 µmol/g DW). Compared to the A12A2 (G) cell line, the CRPP (S) produced 85-fold and 156-fold greater strictosidine and serpentine, respectively. This indicates that a high level of iridoid precursor results in depletion of the indole precursors in the CRPP cell lines, whereas in other cell lines, the iridoid pathway was the limiting factor for TIA production, in accordance with previous reports (Moreno et al. 1993; Whitmer et al. 2002).

The antihypertensive compounds; ajmalicine and serpentine are the common mono-TIA found in *C. roseus* cell cultures. Of the cell lines, both CRPP (G) and CRPP (S) accumulated the greatest levels of serpentine (1.77 – 2.37 µmol/g DW), whereas lower levels of serpentine were detected in A11 (G) (0.05 µmol/g DW) and in both A12A2 cell lines (0.02 – 0.57 µmol/g DW). However, ajmalicine was not detected in any of the cell lines employed in this study, even though the accumulation of this compound in the A12A2 and A11 cell lines has been previously reported (Moreno et al. 1993; Contin et al. 1999; El-Sayed and Verpoorte 2002). Serpentine is formed upon vacuolar peroxidase catalyzed oxidation of ajmalicine, for which enzyme activity has been reported to be 20-fold greater in light grown cultures (Blom et al. 1991). As our cell lines were cultivated under continuous light for many years, it is possible that ajmalicine accumulation in these cell lines has been diverted into serpentine.

The highly valuable antineoplastic bisindole alkaloids; anhydrovinblastine, vinblastine, and vincristine were not detected in any of our cell lines. This is due to the lack of vindoline, one of the building blocks of the bisindole alkaloids. Vindoline is not produced in undifferentiated cell cultures of *C. roseus* because its synthesis requires organization of particular cell types found in the aerial tissues (St-Pierre et al. 1999; Murata and De Luca 2005). Biosynthesis of vindoline involves at least six sequential enzymatic reactions starting from the intermediate tabersonine (El-Sayed and Verpoorte 2007). In this study, only CRPP cell lines accumulated tabersonine, as well as another precursor of the bisindole alkaloids, catharanthine. No significant difference was found between the tabersonine levels of CRPP (G) and CRPP (S) cell lines, whereas the level of catharanthine was 1.6-fold higher in the CRPP (S) cell cultures ($P < 0.05$). However, the accumulation ratios between serpentine, tabersonine, and catharanthine seem to be comparable between CRPP (S) and CRPP (G)

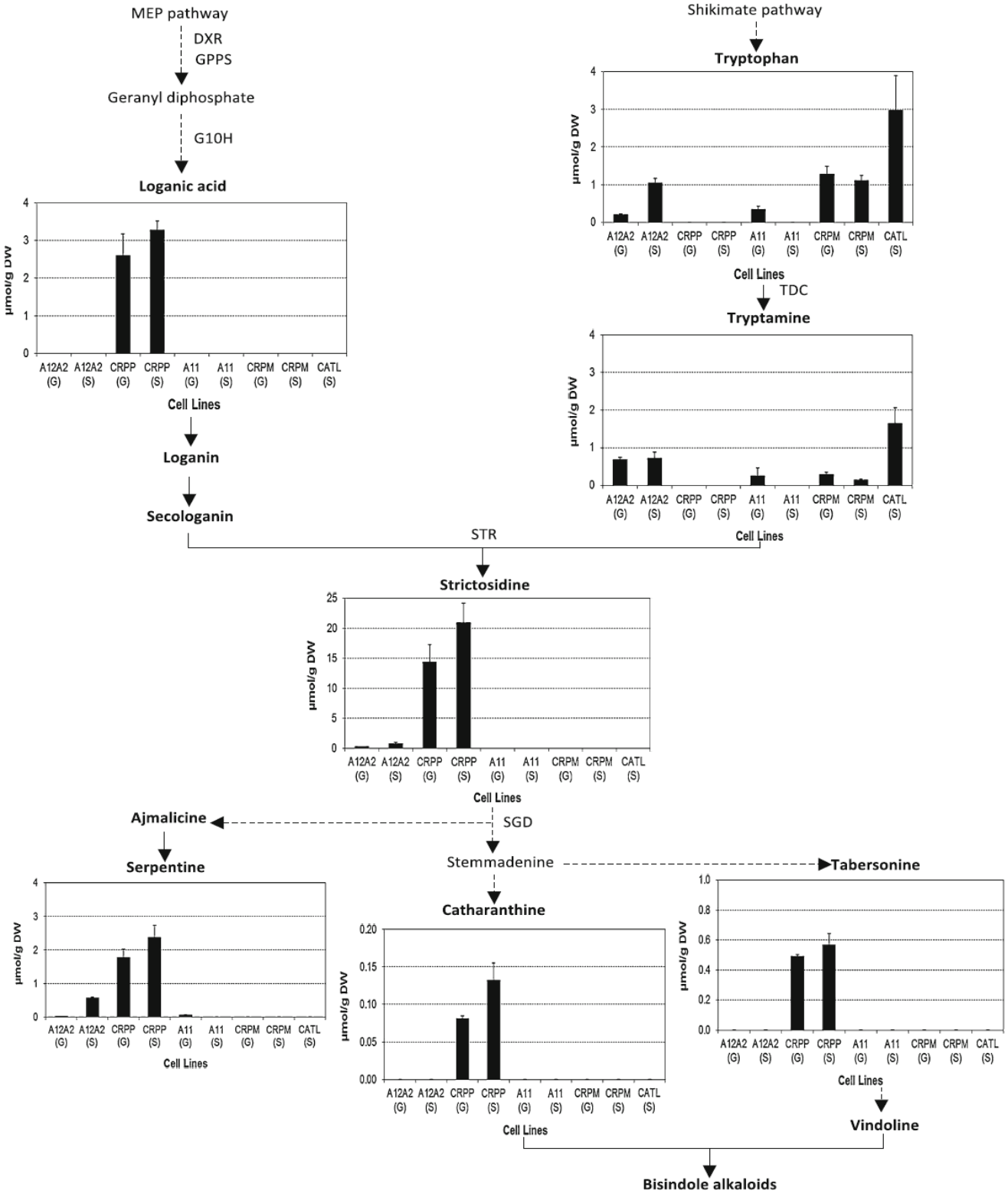

Fig. 2 Analysis of terpenoid indole alkaloids, iridoid and indole precursors in nine *Catharanthus roseus* cell suspension lines. Arrows with dashed lines indicate several biosynthetic steps. DXR: 1-deoxy-D-xylulose-5-phosphate reducto isomerase, GPPS: geranyl diphosphate synthase, G10H: geraniol 10-hydroxylase (G8O: geraniol 8-oxidase), SGD: strictosidine *β*-D-glucosidase, STR: strictosidine synthase, TDC: tryptophan decarboxylase. Error bars represent standard deviation of the mean of three replicates.

lines, i.e. (18:4:1) and (22:6:1), respectively. Apparently, the CRPP cell lines produced greater levels of diverse TIA compared to other cell lines in this study, which makes the CRPP cell lines of a particular interest for bioproduction.

Chung et al. (2011) screened leaves of 64 *C. roseus* cultivars (50 day-old) and showed that 'Cooler Rose Hot' produced the greatest serpentine concentration (1.32 ± 0.13 µmol/g DW). In the present study, the average serpentine concentration of 3 week-old CRPP (G) and CRPP (S) cell lines was 1.77 ± 0.26 µmol/g DW and 2.37 ± 0.36 µmol/g DW, respectively. In addition, the tabersonine levels of the CRPP cell lines (0.49 – 0.57 µmol/g DW) were comparable to that of the 6-week-old Titan Blush cultivar (0.57 µmol/g DW) (Chung et al. 2011). However, the catharanthine level was lower in CRPP cell lines (0.08 – 0.13 µmol/g DW) if compared to the concentrations of the screened *C. roseus* cultivars (0.75 – 8.63 µmol/g DW). The CRPP cell lines accumulated a high level of strictosidine, the first TIA in the biosynthetic pathway. As compared to the 43 *Catharanthus* cultivars analyzed by Hallard (2000), the strictosidine level in the plant leaves was below 5 µmol/g DW, whereas 14.30 µmol/g and 20.87 µmol/g strictosidine were detected in CRPP (G) and CRPP (S) cell lines, respectively.

Analysis of carotenoids

The GGPP pathway towards carotenoid production is a potential competitor for TIA biosynthesis, as both pathways derive from the same precursor (GPP) within the MEP pathway. The accumulation of carotenoids in the *C. roseus* cell suspension lines is shown in **Fig. 3**. Only low levels (< 15 nmol/g DW) of 5,6-epoxy lutein were detected in the CRPM and CATL cell lines, even though its intermediate lutein accumulated at much greater levels in CRPP and A12A2 (S) cell lines ($P < 0.05$). This suggests lutein as the accumulated end-product in this pathway. The earlier precursor of those compounds, i.e. α-carotene, was not detectable in most of the cell lines or detected at trace level (present as tiny peak in the chromatograms) in the CRPP (G) cell line.

In contrast to another pathway, β-carotene was remarkably high in the cell lines, with the trans-β-carotene about 2 – 10 times greater than the *cis*-isomer. Both types of β-carotene as well as the downstream products, violaxanthin and neoxantin, accumulated at greater levels in the A12A2 (S) and both CRPP cell lines ($P < 0.05$) than in the other six cell lines (**Fig. 3**). Zeaxanthin, the intermediate of violaxanthin and neoxanthin, was not detected in

A12A2, CRPP, and A11 cell lines although it was present in low amounts in the CRPM and CATL cell lines. It is presumed that zeaxanthin was fully utilized in A12A2, CRPP, and A11 cell lines to produce violaxanthin and neoxanthin.

The composition of carotenoids in plant leaves is nearly similar in all species: 45% lutein, 25 – 30% *β*-carotene, 15% violaxanthin, 10% neoxanthin, and small amounts of *α*-carotene and zeaxanthin (Namitha and Negi 2010). In our study, *β*-carotene provided the largest part of the composition of carotenoids in *C. roseus* cell suspension cultures, with 88 – 92% in A12A2 and CRPP cell lines, 70 – 78% in CRPM and CATL cell lines, and 48 – 58% in A11 cell lines. Lutein was the second most abundant, with 24 – 26% in the A11 cell lines, 9% in CRPM cell lines, and 5 – 7% in the other cell lines and subsequently, it was followed by neoxanthin and violaxanthin in most of the cell lines.

Analysis of phytosterols

The terpenoid precursor IPP::DMAPP synthesized in the plastidial MEP pathway can be exported to the MVA pathway in the cytosol (Laule et al. 2003). Therefore, the down-stream part of the MVA pathway may also compete with TIA and carotenoid biosynthesis for availability of the central five-carbon (C5) intermediate. In the MVA pathway, plant sterols are synthesized from FPP, which then lead to the production of campesterol via 24-methylenecholesterol or to isofucosterol and subsequently to sitosterol and stigmasterol. Three major phytosterols, i.e. campesterol, stigmasterol, and *β*-sitosterol were analyzed in the *C. roseus* cell lines (**Fig. 4**). In this study, both CRPP cell lines accumulated the greatest levels of campesterol (1.19 – 1.51 µmol/g DW), whereas the lowest level (0.31 µmol/g DW) was in A12A2 (S) ($P < 0.05$). Both A11 cell lines accumulated more *β*-sitosterol than the other cell lines ($P < 0.05$). The lower level of *β*-sitosterol in CRPP (G) seemed to be compensated by a twofold increase in stigmasterol ($P < 0.05$), suggesting an efficient flux towards stigmasterol as accumulated end-product in this cell line. In contrast, little conversion of *β*-sitosterol to stigmasterol was detected in the other cell lines, which resulted in relatively low levels of stigmasterol compared to *β*-sitosterol. In considering the total amount of *β*-sitosterol and stigmasterol versus campesterol, we could deduce that most of the cell lines, i.e. A12A2 (S), CRPP (G), CRPP (S), CRPM (G), and CATL, favored campesterol production, which is in accordance with Suzuki et al. (1995). There were no differences between the levels of campesterol and *β*-sitosterol + stigmasterol in A12A2 (G) and CRPM (S). Although the sum of *β*-sitosterol and stigmasterol levels was greater than campesterol in both A11 cell lines, the results were not statistically significant ($P < 0.05$).

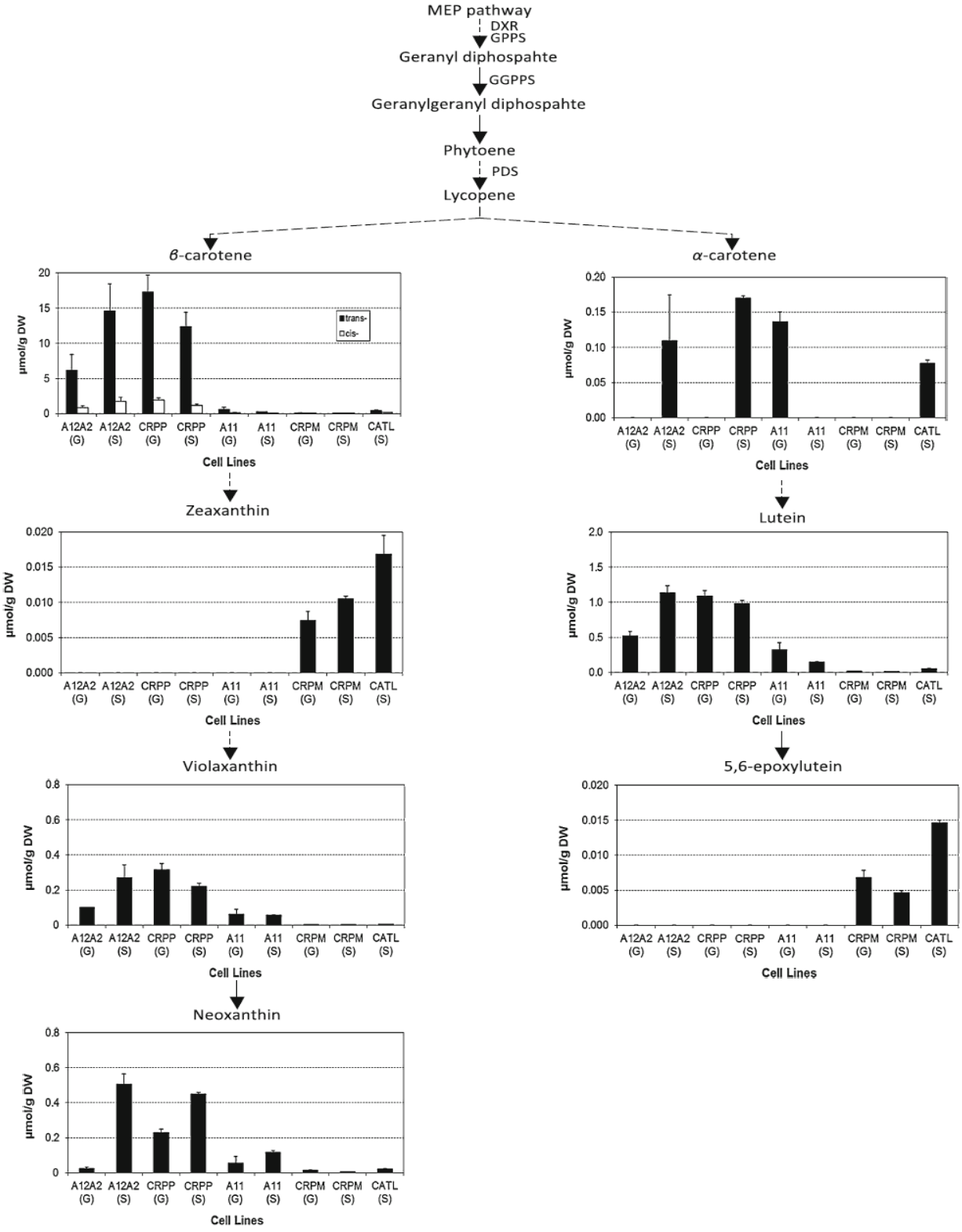

Fig. 3 Carotenoid analysis in nine *Catharanthus roseus* cell suspension lines. Arrows with dashed lines indicate several biosynthetic steps. DXR: 1-deoxy-D-xylulose-5-phosphate reducto isomerase, GPPS: geranyl diphosphate synthase, GGPPS: geranylgeranyl diphosphate synthase, PDS: phytoene desaturase. Error bars represent standard deviation of the mean of three replicates.

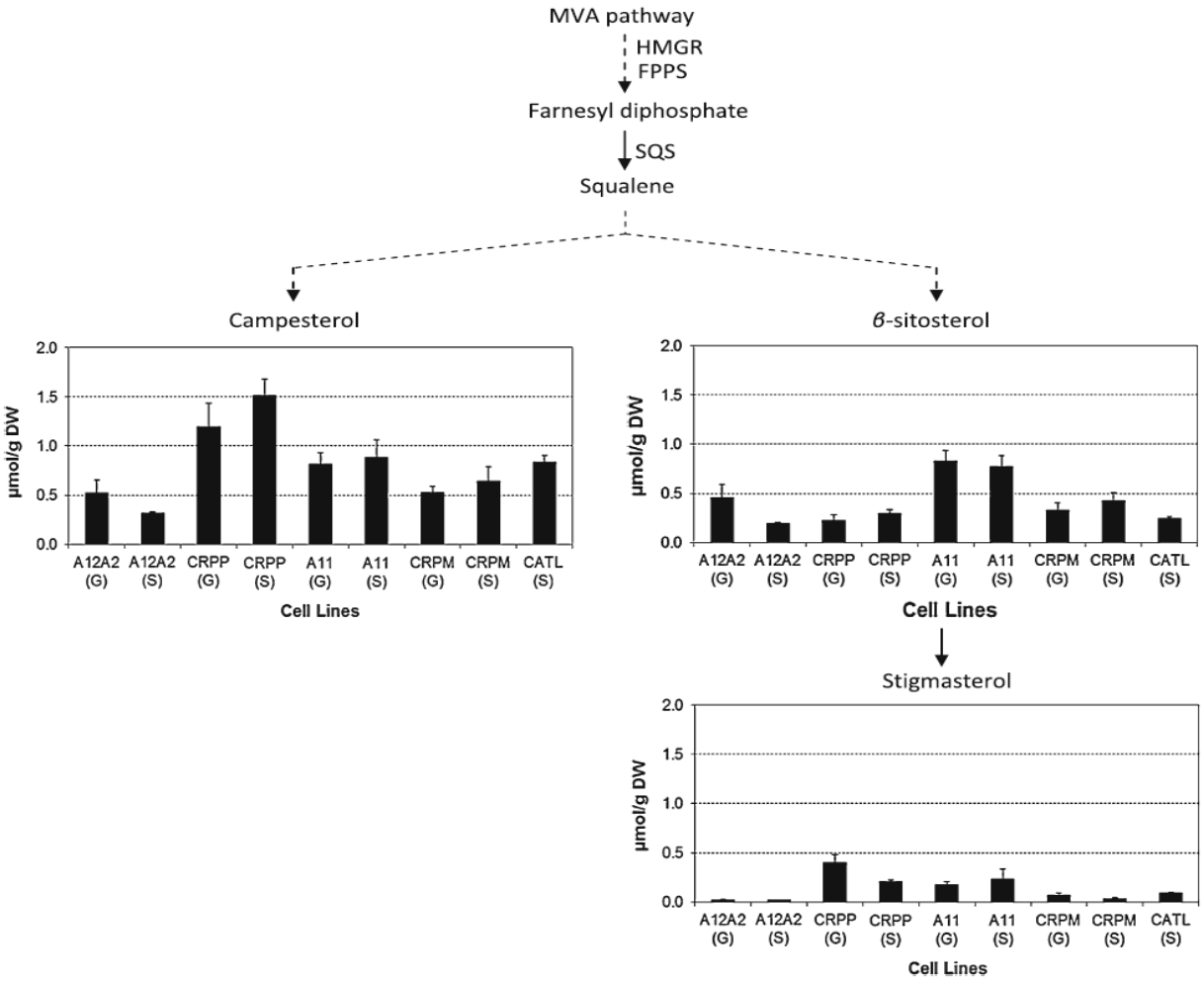

Fig. 4 Sterol analysis in nine *Catharanthus roseus* cell suspension lines. Arrows with dashed lines indicate several biosynthetic steps. HMGR: 3-hydroxy-3-methylglutaryl-CoA reductase, FPPS: farnesyl diphosphate synthase, SQS: squalene synthase. Error bars represent standard deviation of the mean of three replicates.

Total terpenoid accumulation and five-carbon (C5) distribution

Next to analytical evaluation on the individual compounds of TIA, carotenoids, and sterols, the total accumulations of the terpenoid groups were also compared between cell lines (**Fig. 5a**). The TIA level (17 – 24 µmol/g DW) was highly accumulated in CRPP (S) and CRPP (G) cell lines, in which strictosidine provided the largest part of the total TIA composition (86 – 87%). The CRPP cell lines also contained high concentrations of carotenoids (15 – 21 µmol/g DW), whereas the total sterol concentration (1.8 – 2.0 µmol/g DW) was lower than the level of carotenoids and TIA. In A12A2 (G) and A12A2 (S) cell lines, the carotenoid levels were 29- and 14-fold greater, respectively, than those of TIA. In all A11, CRPM, and CATL cell lines, carotenoids were not accumulated more than the levels of sterols. Among the cell lines, CRPP (S) was found to be the most promising TIA-

producing cell line and to have more TIA than carotenoids ($P < 0.05$). Further study needs to be performed to determine whether the terpenoid ratios change at different growth phases. It also remains to be determined whether the TIA:carotenoid ratio can be influenced by external factors, e.g. culture condition and medium composition.

In order to investigate the distribution of five-carbon (C5) precursor in different terpenoid groups from the respective terpenoid biosynthetic pathways, the accumulated levels (in µmol/g DW) of TIA, carotenoids, and sterols were multiplied by the number of C5 units utilized in each group (i.e. TIA = 2 x C5 unit, carotenoid = 8 x C5 unit, and sterol = 6 x C5 unit). The result in **Fig. 5b** shows that the C5 level was greatest in the GGPP pathway towards carotenoid production in all A12A2 and CRPP cell lines. The distribution of C5 was about fourfold (167 µmol/g DW) and twofold (122 µmol/g DW) greater in carotenoids than TIA in CRPP (G) and CRPP (S), respectively. In both CRPP cell lines, the C5 distribution of TIA was significantly greater than sterols ($P < 0.05$). No significant difference of the C5 distribution between TIA and sterols was found in both A12A2 cell lines ($P < 0.05$). Distribution of C5 was three and five times more towards sterols than carotenoids in CRPM (G) and CRPM (S), respectively. A balanced ratio (1:1) of carotenoids:sterols was observed in CATL (S) and A11 (G) cell lines, whereas two times more C5 was distributed into sterols than carotenoids in A11 (S) cell line.

The distribution over the major terpenoid groups measured in this study gives reasonable information of the channeling of C5 into the different terpenoid pathways, even though it is limited in its detail towards other or derived terpenoid groups. Effort had been taken to measure triterpenoids, i.e. *α*-amyrin, *β*-amyrin, and ursolic acid, in the *C. roseus* cell lines. Those compounds were not detected in our cell lines. A group of plant growth regulators, gibberelllins (GAs), are diterpenoids (C20) synthesized in the MEP pathway, which share the same precursor (GPP) with TIA and carotenoids. As a consequence, GAs biosynthesis could be competing with the monoterpenoid (TIA) and tetraterpenoid (carotenoid) pathways. However, GAs were not analyzed in this study. Based on the study performed by Saimoto et al. (1990), the endogenous GA_{12} and GA_{24} detected in the cultured tumor cell of *C. roseus* was 0.08 ng/g FW and 0.4 ng/g FW, respectively. Therefore, if GAs are present at such low levels in our *C. roseus* cell cultures, their biosynthesis is not tapping large amounts of C5 precursor molecules from the total pool if compared with the TIA and carotenoid pathways. However, TIA production might be inhibited at a low level of GAs as Amini et al. (2009) showed an inhibitory effect on ajmalicine accumulation and the down-

regulation of G10H (G8O) gene in the *C. roseus* cell suspension cultures supplied with exogenous gibberellic acid (0.1 – 0.01 µM).

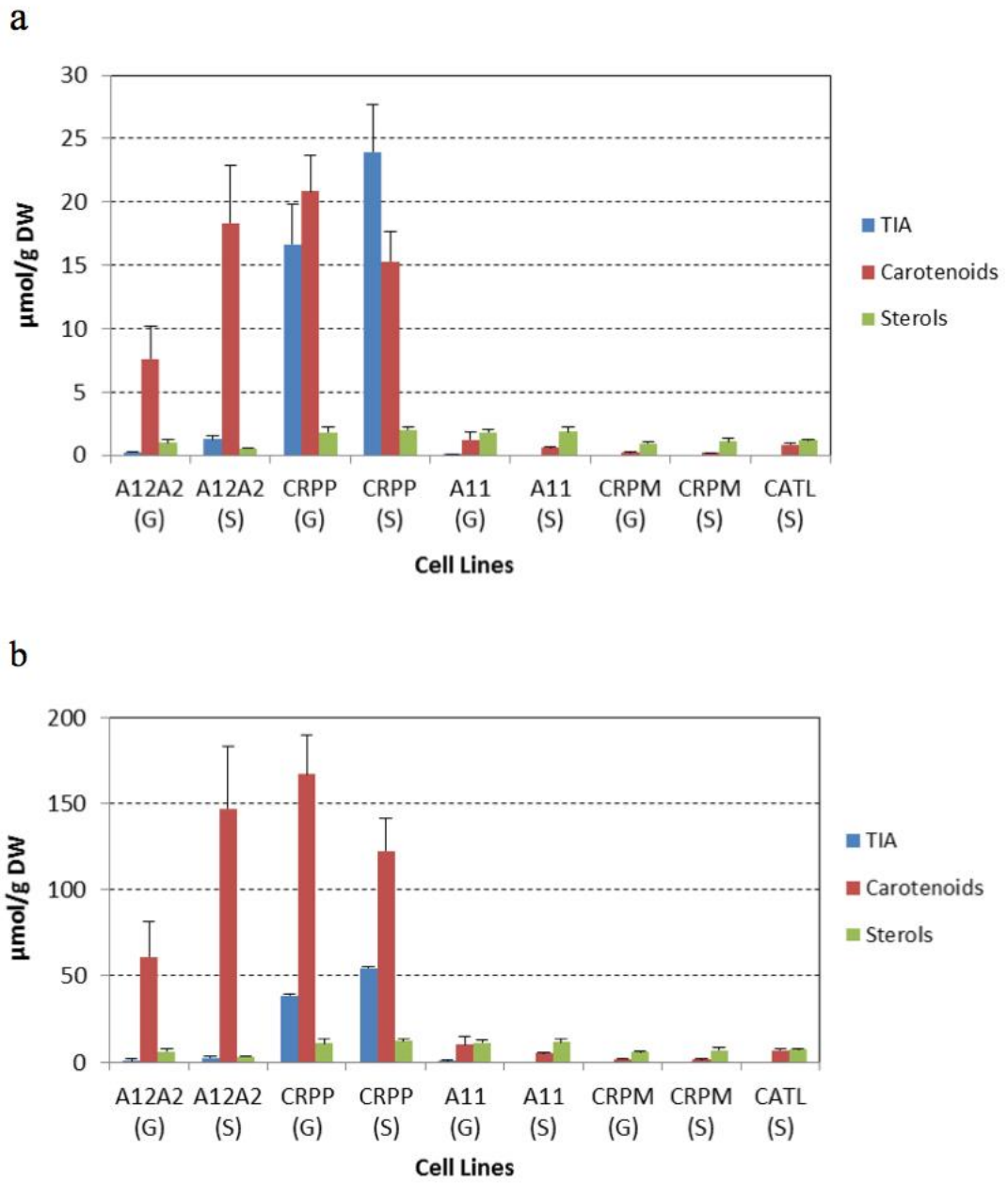

Fig. 5 Total accumulation of terpenoid indole alkaloids, carotenoids, and sterols (a) and distribution of five-carbon (C5) precursor in the respective terpenoid groups (b) in nine *Catharanthus roseus* cell suspension lines. Error bars represent standard deviation of the mean of three replicates.

Cell line characterization using principal component analysis (PCA) and hierarchical cluster analysis (HCA)

In order to distinguish cell lines from one another based on metabolite levels, we applied principal component analysis (PCA) which provides unsupervised clustering method to reduce dimensionality of a multivariate dataset and display systemic variation among samples in an unbiased way. The 18 compounds measured by chromatography are the variables and the observations of the cell lines are based on their µmol/g DW levels. All variables were centered and scaled to unit variance.

The result is presented in a graphical form known as score plot (**Fig. 6a**) and loading plot (**Fig. 6b**). The cell lines were separated by principal component (PC) 1 and 2, which explained 57% and 17% of the variation, respectively. The greatest carotenoid containing cell lines, i.e. CRPP (G), CRPP (S), and A12A2 (S), occurred on the negative side of PC1. The CRPP cell lines accumulating more TIA clustered even more towards the negative side of PC1 than A12A2 (S). The CATL cell line was in the positive quadrant of both PC1 and PC2. According to the loading plot, the CATL could be discriminated from the other cell lines by greater levels of tryptophan, tryptamine, 5,6-epoxy lutein, and zeaxanthin (**Fig. 6b**). Both A11 cell lines were on the positive side of PC1, but on the negative of PC2. These cell lines were characterized by more *β*-sitosterol compared with the other cell lines.

The PCA score plot shows that a cell line grown on a medium with sucrose or glucose cluster closely together, except for the A12A2 cell lines. This suggests that the profiles of observed metabolites of the same type of cell lines are similar and independent of the supplied carbon source. However, the A12A2 (G) and A12A2 (S) cell lines did not group closely which indicates that they differ in their metabolite profiles; we presume that this is mainly due to the difference in the maintenance conditions (see cell line characteristics in **Table 1**). In order to obtain further information on the closeness between groups, we applied hierarchical cluster analysis (HCA) to all component models (9 PCs) from PCA. As shown in **Fig. 6c**, the CRPP-type cell lines which were initiated from a different *C. roseus* cultivar separated into their own group apart from the other cell lines. The CRPM-type cell lines were derived from 58CR cell line, whereas the A12A2 and A11 cell lines derived from the same parental line, i.e. 9CR58, which originated from 58CR cell line. The CATL cell line which clustered close to A12A2 (S) was derived from the A12A2 cell line (**Table 1**). Apparently, the discrimination of the cell lines and the difference in the metabolite profiles could be influenced by both genotype and the cultivation conditions.

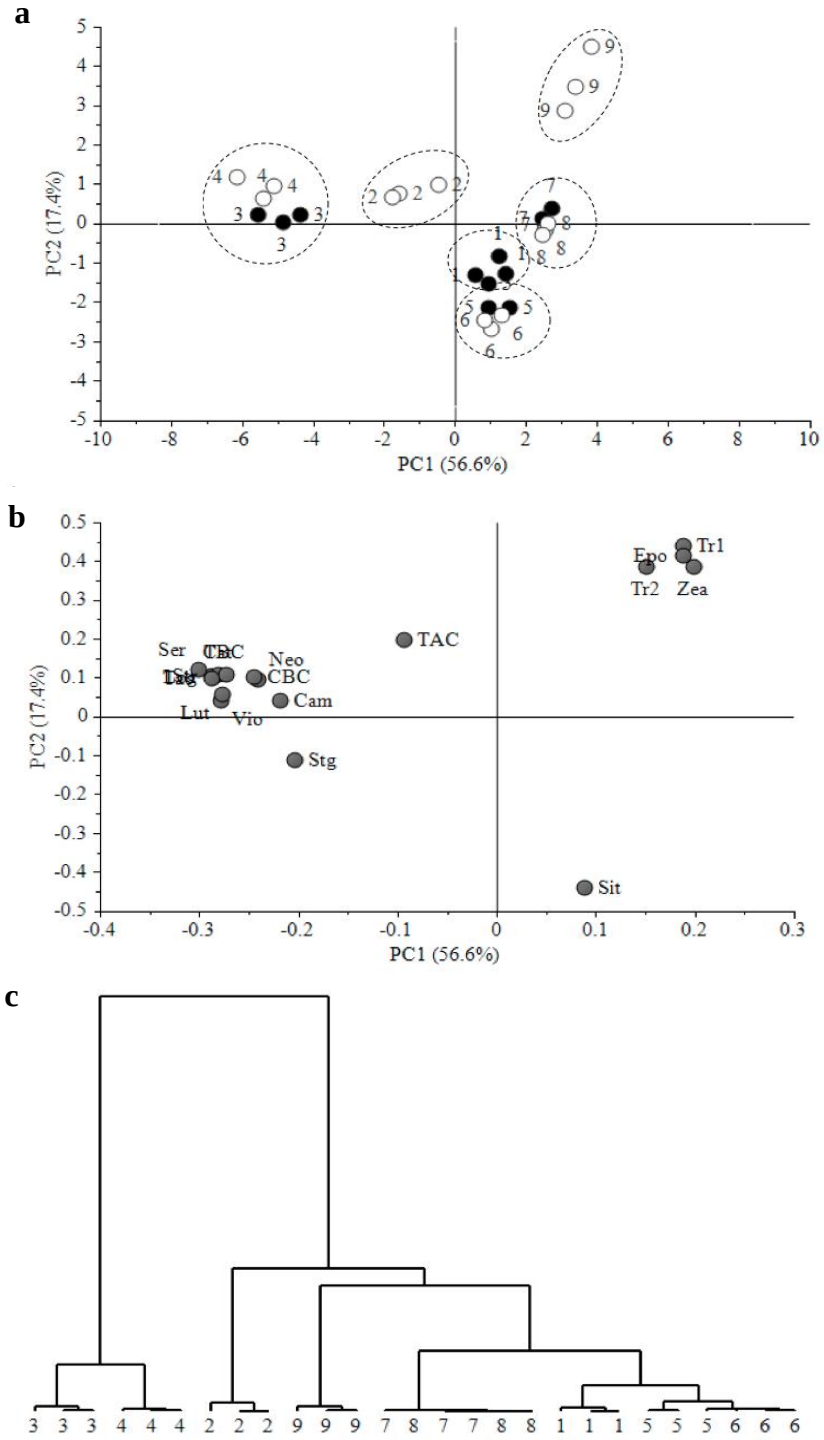

Fig. 6 Principal component analysis (PCA) score (a) and loading (b) plot of nine *Catharanthus roseus* cell suspension lines separated by PC1 and PC2. Dendrogram of hierarchical cluster analysis (HCA) based on nine PCs obtained from PCA (c). 1: A12A2 (G), 2: A12A2 (S), 3: CRPP (G), 4: CRPP (S), 5: A11 (G), 6: A11 (S), 7: CRPM (G), 8: CRPM (S), 9: CATL (S), (○) sucrose, (●) glucose, Tr1: tryptophan, Tr2: tryptamine, Log: loganic acid, Str: strictosidine, Ser: serpentine, Cat: catharanthine, Tab: tabersonine, Cam: campesterol, Stg: stigmasterol, Sit: *β*-sitosterol, Vio: violaxanthin, Neo: neoxanthin, Epo: epoxy-lutein, Lut: lutein, Zea: zeaxanthin, TAC: trans-*α*-carotene, TBC: trans-*β*-carotene, CBC: *cis*-*β*-carotene.

Gene transcript expression

In addition to the metabolite profile, the transcript levels of some genes from the MVA, MEP, and TIA pathways were analyzed from the same samples. The results presented in **Fig. 7** show that both CRPP cell lines expressed geraniol 10-hydroxylase (G10H) gene (also known as geraniol 8-oxidase: G8O) at much greater levels than the other cell lines. The G10H (G8O) enzyme plays a role in catalyzing the conversion of geraniol to 10-hydroxygeraniol (8-hydroxygeraniol), which is an early precursor of the iridoid TIA building block. Collu et al. (2002) showed that G10H (G8O) activity was positively correlated with TIA production. Therefore, it is presumed that the accumulation of loganic acid and TIA in CRPP cell lines was associated with greater transcription levels of G10H (G8O) in the cells. However, a high transcription level does not necessarily represent more enzyme activity, e.g. as availability of cofactors and energy (ATP) are also required. Moreover, the downstream gene transcript levels of loganic acid methyltransferase (LAMT) and secologanin synthase (SLS), which converts loganic acid into loganin and turns loganin into secologanin, respectively, were not measured in this study.

Conversion of tryptophan into tryptamine requires a single enzymatic reaction catalyzed by tryptophan decarboxylase (TDC). The gene transcript level of TDC was highly expressed in the A11 (G) cell line. Whitmer et al. (1998) showed that a high rate of TIA accumulation can occur at low TDC levels and less tryptamine availability which indicate that the rate of TIA biosynthesis depends on rapid turnover of tryptamine rather than on its accumulation, and that high levels of TDC are not required for this rapid turnover to occur. This explains the lack of correlation between TDC activity and TIA biosynthesis. Strictosidine β-D-glucosidase (SGD) is the enzyme converting strictosidine into various TIA. The transcript level of SGD gene was abundant in most of the cell lines, which shows that the cell lines might have high levels of SGD, thus have high capability to produce TIA in the present of substrate.

In the MEP pathway, GPP is converted into GGPP by the enzyme GGPPS. The GGPPS and phytoene desaturase (PDS) are required for carotenoid biosynthesis; the fact that gene transcript levels of both were greater in the CRPP and A12A2 cell lines could link to the high accumulation level of carotenoids in these cell lines. The mRNA levels of 3-hydroxy-3-methylglutaryl-CoA reductase (HMGR) and squalene synthase (SQS) genes associated with sterol biosynthesis in the MVA pathway were greatest in the A11 (G) cell line.

Although the gene transcript profiles in this study show some association with the metabolite profiles, time-course studies for transcriptome and metabolome are needed to

confirm any hypothesis. Previous studies by Dutta et al. (2005) and Chung et al. (2011) reported contradictionary results. Dutta et al. (2005) showed a positive correlation between transcript levels and TIA levels whereas Chung et al. (2011) did not find such a correlation. Therefore, time-course studies could be helpful to gain a better understanding on the association of transcript levels and metabolites, latter of which are usually lag at least 24 hours behind transcription.

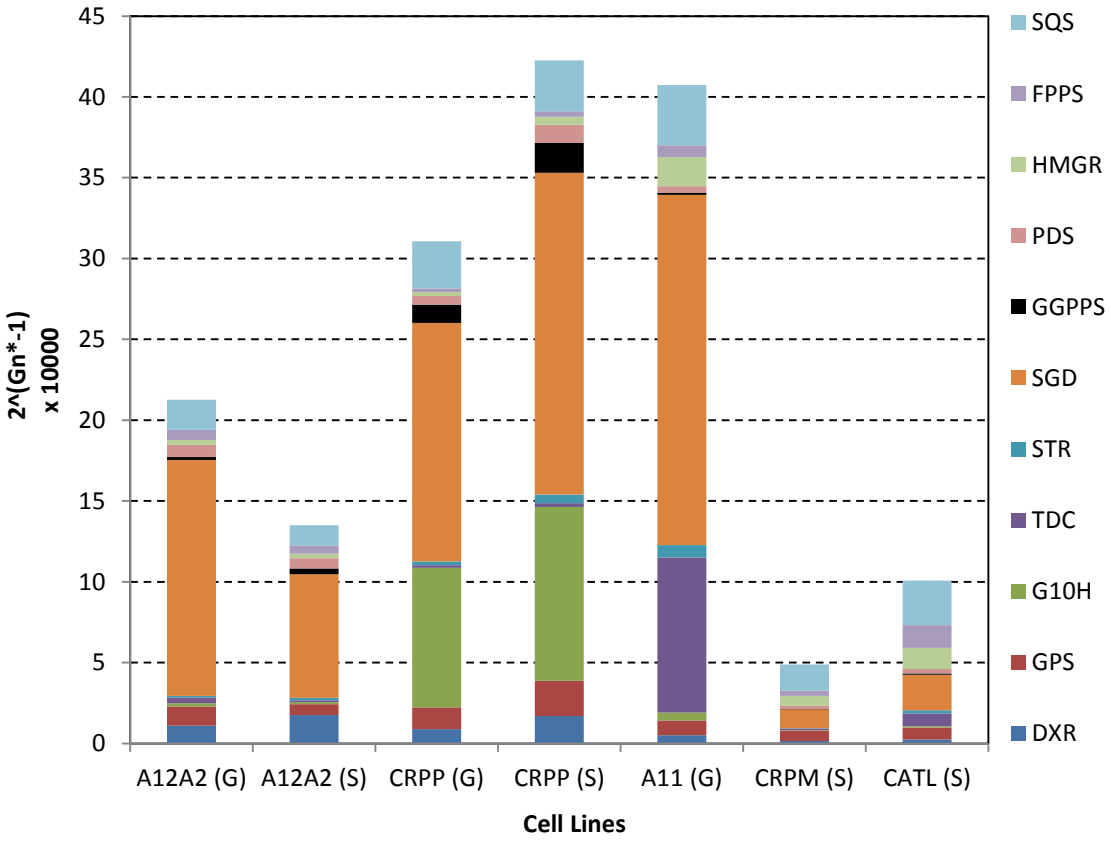

Fig. 7 Transcript levels of some genes from mevalonate (MVA), 2-*C*-methyl-D-erythritol 4-phosphate (MEP), and terpenoid indole alkaloids (TIA) pathways in different *Catharanthus roseus* cell suspension lines. DXR: 1-deoxy-D-xylulose-5-phosphate reducto isomerase, FPPS: farnesyl diphosphate synthase, G10H: geraniol 10-hydroxylase (also known as G8O: geraniol 8-oxidase), GPPS: geranyl diphosphate synthase, GGPPS: geranylgeranyl diphosphate synthase, HMGR: 3-hydroxy-3-methylglutaryl-CoA reductase, PDS: phytoene desaturase, SGD: strictosidine *β*-D-glucosidase, SQS: squalene synthase, STR: strictosidine synthase, TDC: tryptophan decarboxylase.

Conclusion

This study compares the levels of TIA (monoterpenoid) with carotenoids (tetraterpenoid) and sterols (triterpenoid) in several *C. roseus* cell suspension lines. The CRPP (S) cell line showed to be the best TIA-producing cell line and had the best C5

distribution ratio (1:2) between TIA and carotenoids. The production of the latter could be a strong competitor for TIA biosynthesis as both pathways derive from the same precursor (GPP) coming from the MEP pathway. The starting point for monoterpenoid biosynthesis is the geraniol derived from GPP. Increasing the flux from GPP towards geraniol, and thus reduce the production of GGPP, may improve TIA levels in *C. roseus* cell cultures. Sterol production is lower in terms of utilization of the C5 precursors if compared to the TIA and carotenoid in CRPP cell lines. Moreover, even though cross-talk between the pathways may occur at the C5 level, sterols are mainly derived from the mevalonate pathway, and for increasing the flux of precursors to the TIA pathway the sterol pathway seems of less interest.

PCA is useful to chemically distinguish cell lines from each other using quantitative data of metabolite levels. HCA can further refine information on the relationship between cell lines. Higher G10H (or G8O) gene expression levels in the CRPP cell lines seem to be associated with greater TIA accumulation. Nevertheless, time-course studies will be required for a better understanding of this aspect. The metabolite profiles of each cell line are essential not only for information on their chemical composition, but also for better selection of cell lines destined for studies to engineer the terpenoid pathway or to examine interactions of the compounds of interest after a particular treatment of the cell cultures.

Acknowledgements

The authors thank Mr. L. Verhagen (Prisna B.V., Leiden, The Netherlands) for assistance with sterol analysis. The authors also thank the Ministry of Education, Malaysia and University of Malaya, Kuala Lumpur, Malaysia for financial support of Mohd Zuwairi Saiman. This research was funded by the IBOS-ACTS program as coordinated by NWO.

References

Amini A, Glévarec G, Andreu F, Rideau M, Crèche J (2009) Low levels of gibberellic acid control the biosynthesis of ajmalicine in *Catharanthus roseus* cell suspension cultures. Planta Med 75: 187–191

Ben-Amotz A, Lers A, Avron M (1988) Stereoisomers of *β*-carotene and phytoene in the alga *Dunaliella bardawil*. Plant Physiol 86: 1286–1291

Bino RJ, de Vos RCH, Lieberman M, Hall RD, Bovy A, Jonker HH, Tikunov Y, Lommen A, Moco S, Levin I (2005) The light-hyperresponsive *high pigment-2^{dg}* mutation of tomato: alterations in the fruit metabolome. New Phytol 166: 427–438

Blom TJM, Sierra M, van Vliet TB, Franke-van Dijk MEI, de Koning P, van Iren F, Verpoorte R, Libbenga KR (1991) Uptake and accumulation of ajmalicine into isolated vacuoles of cultured cells of *Catharanthus roseus* (L.) G. Don. and its conversion into serpentine. Planta 183: 170–177

Chung IM, Kim EH, Li M, Peebles CAM, Jung WS, Song HK, Ahn JK, San KY (2011) Screening 64 cultivars *Catharanthus roseus* for the production of vindoline, catharanthine, and serpentine. Biotechnol Prog 27: 937–943

Collu G, Garcia AA, van der Heijden R, Verpoorte R (2002) Activity of the cytochrome P450 enzyme geraniol 10-hydroxylase and alkaloid production in plant cell cultures. Plant Sci 162: 165–172

Contin A, Collu G, van der Heijden R, Verpoorte R (1999) The effects of phenobarbital and ketoconazole on the alkaloid biosynthesis in *Catharanthus roseus* cell suspension cultures. Plant Physiol Biochem 37: 139–144

Courdavault V, Burlat V, St-Pierre B, Giglioli-Guivarc'h N (2005) Characterisation of CaaX-prenyltransferases in *Catharanthus roseus*: relationships with the expression of genes involved in the early stages of monoterpenoid biosynthetic pathway. Plant Sci 168: 1097–1107

Dutta A, Batra J, Pandey-Rai S, Singh D, Kuar S, Sen J (2005) Expression of terpenoid indole alkaloid biosynthethic pathway genes corresponds to accumulation of related alkaloids in *Catharanthus roseus* (L.) G. Don. Planta 220: 376–383

El-Sayed M, Verpoorte R (2002) Effect of phytohormones on growth and alkaloid accumulation by a *Catharanthus roseus* cell suspension cultures fed with alkaloid precursors tryptamine and loganin. Plant Cell Tiss Org Cult 68: 265–270

El-Sayed M, Verpoorte R (2007) *Catharanthus* terpenoid indole alkaloids: biosynthesis and regulation. Phytochem Rev 6: 277–305

Gamborg OL, Miller RA, Ojima K (1968) Nutrient requirements of suspension cultures of soybean root cells. Exp Cell Res 50: 155–158

Glenn WS, Runguphan W, O'Connor SE (2013) Recent progress in the metabolic engineering of alkaloids in plant systems. Curr Opin Biotechnol 24: 354–365

Hallard DAC (2000) Transgenic plant cells for the production of indole alkaloids. PhD Thesis, Leiden University, The Netherlands. Chapter 7, Extraction and liquid chromatography photodiode array detection tandem mass spectrometry analysis of *Catharanthus* alkaloids, pp. 88–109. ISBN 9074538495

Hemmerlin A, Hoeffler JF, Meyer O, Tritsch D, Kagan IA, Grosdemange-Billiard C, Rohmer M, Bach TJ (2003) Cross-talk between the cytosolic mevalonate and the plastidial methylerythritol phosphate pathways in tobacco bright yellow-2 cells. J Biol Chem 278: 26666–26676

Laule O, Fürholz A, Chang H-S, Zhu T, Wang X, Heifetz PB, Gruissem W, Lange BM (2003) Crosstalk between cytosolic and plastidial pathways of isoprenoid biosynthesis in *Arabidopsis thaliana*. Proc Natl Acad Sci USA 100: 6866–6871

Moreno PRH, van der Heijden R, Verpoorte R (1993) Effect of terpenoid precursor feeding and elicitation on formation of indole alkaloids in cell suspension cultures of *Catharanthus roseus*. Plant Cell Rep 12: 702–705

Moreno PRH, van der Heijden R, Verpoorte R (1995) Cell and tissue cultures of *Catharanthus roseus*: a literature survey II. Updating from 1988 to 1993. Plant Cell Tiss Organ Cult 42:1–25

Murashige T, Skoog F (1962) A revised medium for rapid growth and bioassays with tobacco tissue cultures. Physiol Plant 15: 473–497

Murata J, De Luca V (2005) Localization of tabersonine 16-hydroxylase and 16-OH tabersonine-16-*O*-methyltransferase to leaf epidermal cells defines them as a major site of precursor biosynthesis in the vindoline pathway in *Catharanthus roseus*. Plant J 44: 581–594

Mustafa NR, Kim Hye Kyong, Choi YH, Verpoorte R (2009) Metabolic changes of salicylic acid-elicited *Catharanthus roseus* cell suspension cultures monitored by NMR-based metabolomics. Biotechnol Lett 31: 1967–1974

Mustafa NR, Verpoorte (2007) Phenolic compounds in *Catharanthus roseus*. Phytochem Rev 6: 243–258

Mustafa NR, de Winter W, van Iren F, Verpoorte R (2011) Initiation, growth and cryopreservation of plant cell suspension cultures. Nat Protoc 6: 715-742

Namitha KK, Negi PS (2010) Chemistry and biotechnology of carotenoids. Crit Rev Food Sci Nutr 50: 728–760

O'Connor SE (2012) Strategies for engineering plant natural products: the iridoid-derived monoterpene indole alkaloids of *Catharanthus roseus*. Methods Enzymol 515: 189–206

Pati PK, Kaur J, Singh P (2011) A liquid culture system for shoot proliferation and analysis of pharmaceutically active constituents of *Catharanthus roseus* (L.) G. Don. Plant Cell Tiss Organ Cult 105: 299–307

Pietrosiuk A, Furmanowa M, Łata B (2007) *Catharanthus roseus*: micropropagation and in vitro techniques. Phytochem Rev 6: 459–473

Rohmer M (1999) The discovery of a mevalonate-independent pathway for isoprenoid biosynthesis in bacteria, algae and higher plants. Nat Prod Rep 16: 565–574

Salim V, De Luca V (2013) Towards complete elucidation of monoterpene indole alkaloid biosynthesis pathway: *Catharanthus roseus* as a pioneer system. In: Giglioli-Guivarc'h N (ed.) Advances of Botanical Research – New Light on Alkaloid Biosynthesis and Future Prospects, Academic Press, London, pp. 1–37

Saimoto H, Nakagawa S, Kobayashi M, Fujioka S, Barreto MCC, Sakurai A, Syono K (1990) Endogenous levels of gibberellins, IAA and cytokinins in *Catharanthus* crown gall tissues of different tumor types. Plant Cell Physiol 31: 365–370

Schuhr CA , Radykewicz1 T, Sagner S, Latzel C, Zenk MH, Arigoni D, Bacher A, Rohdich F, Eisenreich W (2003) Quantitative assessment of crosstalk between the two isoprenoid biosynthesis pathways in plants by NMR spectroscopy. Phytochem Rev 2: 3–16

Suzuki H, Inoue T, Fujioka S, Saito T, Takatsuto S, Yokota T, Murofushi N, Yanagisawa T, Sakurai A (1995) Conversion of 24-methylcholesterol to 6-oxo-24-methylcholestanol, a putative intermediate of the biosynthesis of brassinosteroids, in cultured cells of *Cathanranthus roseus.* Phytochemistry 40: 1391–1397

St-Pierre B, Vazquez-Flota F, De Luca V (1999) Multicellular compartmentation of *Catharanthus roseus* alkaloid biosynthesis predicts intercellular translocation of pathway intermediate. Plant Cell 11: 887–900

Taylor RF, Farrow PE, Yelle LM, Harris JC, Marenchic IG (1990) Advances in HPLC and HPLC-MS of carotenoids and retinoids. In: Krinsky NI, Mathews-Roth MM, Taylor RF (eds.) Carotenoids: Chemistry and Biology, Plenum Press, New York, pp. 105–123

Tikhomiroff C, Jolicoeur M (2002) Screening of *Catharanthus roseus* secondary metabolites by high-performance liquid chromatography. J Chromatogr A 955: 87–93

van der Heijden R, Jacobs DI, Snoeijer W, Hallard D, Verpoorte R (2004) The *Catharanthus* alkaloids: pharmacognosy and biotechnology. Curr Med Chem 11: 607– 628

Verpoorte R, Contin A, Memelink J (2002) Biotechnology for the production of plant secondary metabolites. Phytochem Rev 1: 13–25

Whitmer S, Canel C, Hallard D, Goncalves C, Verpoorte R (1998) Influence of precursor availability on alkaloid accumulation by transgenic cell line of *Catharanthus roseus*. Plant Physiol 116: 853–857

Whitmer S, van der Heijden R, Verpoorte R (2002) Effect of precursor feeding on alkaloid accumulation by a strictosidine synthase over-expressing transgenic cell line S1 of *Catharanthus roseus*. Plant Cell Tiss Organ Cult 69: 85–93

Zhao J, Verpoorte R (2007) Manipulating indole alkaloid production by *Catharanthus roseus* cell cultures in bioreactors: from biochemical processing to metabolic engineering. Phytochem Rev 6: 435– 457

Zhou ML, Shao JR, Tang YX (2009) Production and metabolic engineering of terpenoid indole alkaloids in cell cultures of the medicinal plant *Catharanthus roseus* (L.) G. Don (Madagascar periwinkle). Biotechnol Appl Biochem 52: 313–323

Supplement 1 List of primers for quantitative RT-PCR

Gene	Product size (bp)	Primer sequences	
	cDNA	Forward	Reverse
HMGR	162	5′-GAGATGGAATGACTAGGGCTCC-3′	5′-GCAATTGCACATTGGACGCT-3′
DXR	147	5′-TTGGCCCCGCCTTGATCTTT-3′	5′-GCCTTCTCATTTGCTGCACT-3′
GPS	299	5′-TGAAACAAGGCGAGGGATTG-3′	5′-GATGTTTGCCCAGCAAGAAG-3′
PDS	309	5′-GCAGTTGGACTCTTGCCG-3′	5′-GCACTTCACCTCCTAGTGATCG-3′
GGPPS	264	5′-ATGCGCTCTAATCTTTGTCACCC-3′	5′-CCCTAACCAAGACTGCATCTTCC-3′
G10H (G8O)	247	5′-GGTAGCCTCACGATGGAGAA-3′	5′-CCTTGGCAGAATCCGAATAA-3′
TDC	227	5′-CGCCTGTATATGTCCCGAGT-3′	5′-GTTGCGATTTGCCAATTTTT-3′
SGD	246	5′-ATTTGCACCAGGAAGAGGTG-3′	5′-TATGAACCATCCGAGCATGA-3′
FPPS	160	5′-GGCTGGTTGTGAAAGCATTAG-3′	5′-CTCAAACACACCCTGAAGATCAAG-3′
SQS	265	5′-TATTTGGTTCTTCGAGCTCTTGACAC-3′	5′-ATATTTCGATTCTGTGCTATTCCACA-3′
STR	146	5′-TGCCACACAACTAGCCACAA-3′	5′-TCATGATTTCTTCCACACCTTCG-3′
Rsp9	190	5'-TCCACCATGCCAGAGTGCTCATTAGG-3′	5'-TCCATCACCACCAGATGCCTTCTTCG-3'